Sensors & Diagnostics

PAPER

View Article Online
View Journal | View Issue



Cite this: *Sens. Diagn.*, 2026, **5**, 730

# A non-invasive blister fluid-based rapid test for point-of-care detection of varicella and herpes zoster: preliminary validation in a clinical setting

Fang-Ying Wang, [ab] Yi-You Huang*[c] and Chao-Min Cheng *[d]

Received 19th December 2025,
Accepted 11th March 2026

DOI: 10.1039/d5sd00231a

rsc.li/sensors

Varicella and herpes zoster, caused by varicella-zoster virus (VZV), remain prevalent worldwide and can cause severe complications if diagnosis is delayed. Early detection within the 72-hour therapeutic window is essential for initiating antiviral therapy to reduce transmission, postherpetic neuralgia, and other complications. Few non-invasive point-of-care tests for VZV are currently available. In this preliminary clinical validation of 30 cases, we developed and evaluated a blister fluid-based lateral flow immunoassay for rapid VZV detection. The assay was tested using VZV standard solutions and blister fluid from patients and healthy controls. In real-world testing, direct visual interpretation achieved 80% sensitivity and 100% specificity within 15 minutes. Reflectance spectral analysis enabled quantitative measurement, with a limit of detection of 1.48 pg $mL^{-1}$ and a limit of quantitation of 42.9 pg $mL^{-1}$; smartphone-assisted analysis produced comparable results without laboratory equipment. Its rapid turnaround, non-invasive sampling, and portability make this approach suitable for diverse healthcare settings, including community-based and at-home use. This "blister fluid biopsy" strategy may facilitate timely intervention, improve patient outcomes, and strengthen infection control, particularly in resource-limited environments.



## Introduction

Varicella and herpes zoster, both caused by the varicella-zoster virus (VZV), remain significant global health concerns despite advances in vaccination programs. Primary VZV infection manifests as varicella (chickenpox), characterized by diffuse vesicular, pustular, and crusted eruptions accompanied by fever.[1] Following resolution, the virus establishes lifelong latency in sensory ganglia. Endogenous reactivation results in herpes zoster (shingles), a debilitating condition typified by grouped vesicles along one or adjacent dermatomes, often accompanied by severe radicular pain. In many patients, this pain persists beyond rash resolution, progressing to postherpetic neuralgia (PHN). PHN causes considerable patient suffering and is challenging to treat in clinical practice.[2] Beyond PHN, herpes zoster can cause vision-threatening herpes zoster ophthalmicus and acute retinal necrosis.[3] Involvement of the geniculate ganglion causes facial paralysis and Ramsay Hunt syndrome, which is often associated with hearing loss, nausea, and nystagmus.[4] In immunocompromised individuals, both varicella and herpes zoster can disseminate, involving the lungs, liver, or central nervous system, and may be fatal.[4,5] Timely identification and intervention are therefore essential to halt viral replication, limit inflammation, and prevent irreversible sequelae.

Before the introduction of varicella vaccination, varicella was a significant cause of morbidity and mortality worldwide.[6,7] Although the introduction of varicella vaccination has markedly reduced disease burden, VZV remains prevalent in clinical practice. The lifetime risk of herpes zoster is approximately one in three,[8] and vaccine efficacy is reduced in high-risk groups and may even be a possible infection source because VZV vaccines contain attenuated live viruses.[9] VZV is highly contagious, with a secondary attack rate of approximately 90% among susceptible household contacts,[10] and transmission can occur *via* direct contact, respiratory droplets, or aerosols from vesicular fluid.[1] Critically, there is no standardized, point-of-care method to determine contagiousness—a gap with major public health implications for protecting unvaccinated infants and immunocompromised individuals.

In routine dermatologic practice, the diagnosis of VZV infection is primarily based on clinical examination. However, early-stage lesions can present atypically, mimicking other blistering disorders such as herpes simplex

[a] *Department of Dermatology, Chang Gung Memorial Hospital, Linkou Medical Center, Taoyuan, Taiwan*
[b] *College of Medicine, Chang Gung University, Taoyuan, Taiwan*
[c] *Department of Biomedical Engineering, College of Medicine, College of Engineering, National Taiwan University, Taipei, Taiwan. E-mail: yyhuang@ntu.edu.tw*
[d] *Institute of Biomedical Engineering, National Tsing Hua University, Hsinchu, Taiwan. E-mail: chaomin@mx.nthu.edu.tw*

virus (HSV) infection, bullous impetigo, bullous pemphigoid, pemphigus vulgaris, bullous contact dermatitis, or trauma-related blisters.[11] Reliance on visual inspection alone often compels clinicians either to monitor the rash until further evolution or to request confirmatory laboratory testing—such as polymerase chain reaction (PCR), direct immunofluorescence, or viral culture—that is inherently time-consuming and dependent on specialized equipment and trained personnel. Such delays not only risk missing the optimal therapeutic window for antiviral therapy, which achieves the greatest benefit when initiated within 72 hours of rash onset,[12,13] but also may permit viral replication to continue without timely suppression, thereby heightening the risk of severe complications, prolonging the duration of pain, and facilitating further transmission.[14] Conversely, misdiagnosis can lead to harmful interventions; for instance, administration of high-dose corticosteroids for presumed bullous autoimmune or allergic disease can cause widespread viral dissemination.

To address this urgent diagnostic gap, we developed a rapid, laboratory-free lateral flow immunoassay for VZV antigen detection using blister fluid. In this pilot study, we evaluated the analytical performance and clinical feasibility of this platform in patients with vesiculobullous disorders. In addition to direct visual interpretation, quantitative readout modalities—including reflectance spectral analysis and smartphone-based colorimetry—were explored to enhance objectivity and adaptability across diverse healthcare settings. The simplicity, non-invasive sampling strategy, and portability of this approach position it as a potential point-of-care tool for varicella and herpes zoster diagnosis. Furthermore, the concept of a "blister fluid biopsy" introduces a practical framework for leveraging lesion-derived fluid in dermatologic diagnostics. This preliminary validation provides a foundation for future large-scale studies and broader translational applications.

## Materials and methods

### Preparation of VZV rapid test strips

It has been shown that the glycoprotein E (gE)–glycoprotein I (gI) complex of varicella-zoster virus (VZV) is essential for viral replication and facilitates intercellular transmission.[15] As illustrated in Fig. 1, the paper-based test strips were fabricated using a lateral flow immunoassay (LFA) platform.[16] Twenty mL of a commercially obtained colloidal gold nanoparticle suspension (40 nm; ab269930, Abcam, Cambridge, UK) was adjusted to pH 8.0 ± 0.1 with 0.1 M sodium borate buffer and incubated with 0.3 mL of anti-VZV gE monoclonal antibody (clone 9, 0.2 mg $mL^{-1}$; GeneTex, Cat# GTX64187) for 1 hour under gentle stirring, followed by blocking with 2.0 mL of 10% bovine serum albumin (BSA) for another hour. The conjugate was stored overnight at 2–8 °C, centrifuged to achieve ~10× concentration, and resuspended for use as the gold–antibody detection probe in the LFA system. The nitrocellulose membrane was pre-coated with a capture antibody by dispensing vertical test (T) lines containing anti-VZV gI monoclonal antibody (clone 3B3, EMD Millipore, Cat# MAB8612, Burlington, MA, USA), which specifically binds the VZV antigen–antibody–gold complexes.

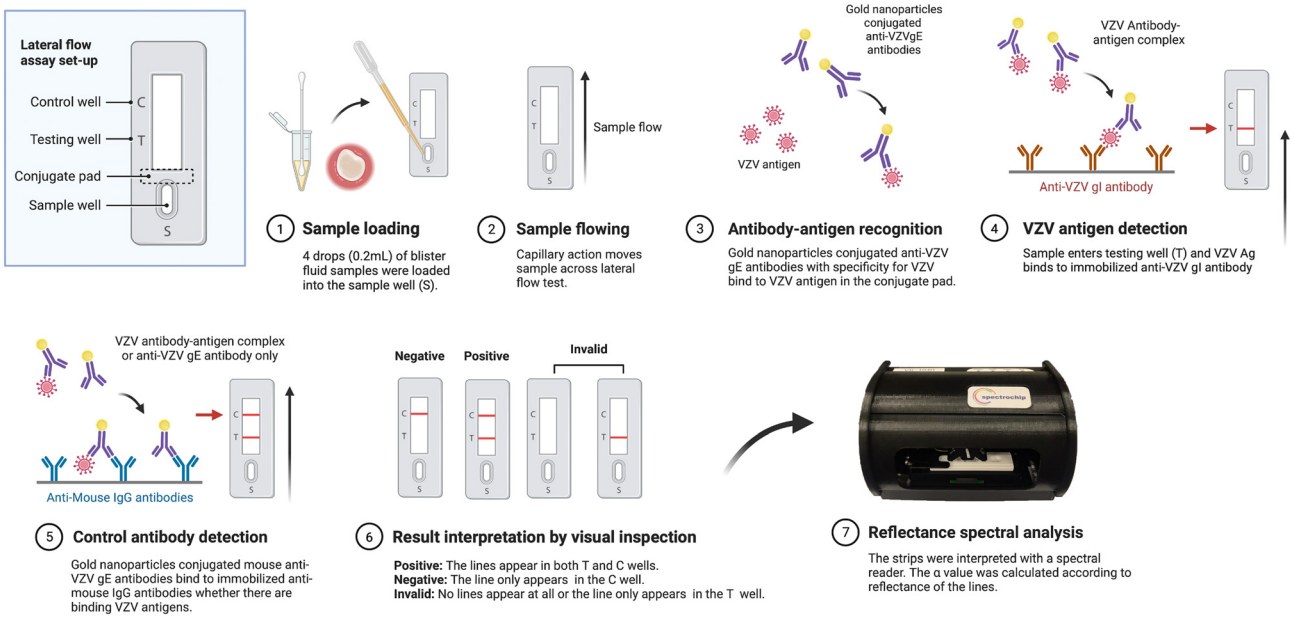


**Fig. 1** Workflow and interpretation of VZV rapid test strips. When the blister fluid sample was loaded and allowed to flow along the strip (1 and 2), the sample with VZV antigen formed an antigen–antibody complex with the colloidal nanogold-conjugated anti-VZV-gE antibody (3). These antigen–antibody complexes were then captured by anti-VZV-gI antibodies on the T-line area of the test strip, and then appeared as a colored T-line (4). The anti-mouse IgG antibodies on the C-line capture the nanogold-conjugated anti-VZV-gE antibody, so all valid strips would show a colored C-line (5). After direct visual interpretation (6), the strips were analyzed with a reflectance spectral reader (7).

The control (C) line was coated with goat anti-mouse IgG (Arista Biologicals, Inc., USA) along with quality-control antibodies to ensure assay validity.

During testing, capillary action enabled the blister-fluid sample to migrate laterally across the strip, allowing VZV antigens to form immune complexes with the gold–antibody conjugates on the conjugate pad. These complexes were subsequently captured by the immobilized anti-VZV gI antibodies at the T line, producing a visible colored band. Independent of antigen presence, the anti-mouse IgG antibodies at the C line bound excess gold conjugates, thereby generating a control band to confirm suitable test function. The assembled test strips were air-dried, individually packaged with desiccants, and stored under dry conditions at room temperature until use.

### *In vitro* test and reflectance spectral quantitative analysis

To characterize the analytical performance of the developed VZV rapid test strip, *in vitro* reflectance spectral analysis was performed using serially diluted varicella zoster virus (VZV) glycoprotein antigen (Strain Ellen, native, HEL-299 cell culture; Jena Bioscience, Cat. No. PR-BA104VSG-S). For calibration, the VZV glycoprotein antigen was diluted with phosphate-buffered saline (PBS, pH 7.4) to generate a concentration range of 0–800 pg $mL^{-1}$, which encompassed the expected clinical levels in vesicular fluid. Each dilution (100 μL) was applied to the sample well of the VZV test strip, and results were measured after lateral flow completion (15 minutes). Reflectance spectra were obtained using a spectrum analyzer (in cooperation with Taiwan SpectroChip Inc.; Taiwan FDA registration: MD(I)-008090; US FDA registration: 3017810861), which provided continuous spectrum results and captured high-resolution reflectance spectrum values from the T-line of the strip. When scanning with white light, the colloidal gold absorbed the spectrum at 430 and 600 nm wavelengths and reflected the remaining light. Colloidal gold does not absorb light at a 650 nm wavelength, so we used that wavelength as the reflection wavelength for our reader. The ratio of the reflectance to the spectrum at the reference wavelength was used to calculate the $\alpha$ value: $\alpha$ = reflectance (650 nm)/reflectance (the minimum value in the range of 430–600 nm). In this formula, the $\alpha$ value refers to the color reflection of the optical scanning VZV rapid test strip. Higher $\alpha$ values corresponded to stronger reflection intensities of the VZV antigen–antibody–colloidal gold complex, indicating higher antigen concentration.[17]

A linear regression model was constructed to evaluate the correlation between $\alpha$ values and antigen concentrations. The limit of detection (LOD) and limit of quantification (LOQ) could be estimated based on the average of the blank $\alpha$ value, the standard deviation of the blank $\alpha$ value, the slope of the calibration curve, and the defined confidence factor, by the following formula, respectively: LOD = blank (mean) + 3 × blank (standard deviation) and LOQ = blank (mean) + 10 × blank (standard deviation). Each concentration was tested in triplicate, and mean $\alpha$ values were used for regression analysis. The derived regression equation was subsequently used to estimate viral antigen levels in patient blister fluid samples. For intra-assay reproducibility, each VZV antigen concentration was tested in triplicate within a single analytical run. The mean, standard deviation, and coefficient of variation (CV%) were calculated for each concentration, with CV% values serving as indicators of measurement repeatability.

### Clinical validations

To validate the diagnostic performance of the VZV rapid test in a real-world clinical setting, 30 participants with vesiculobullous disorders were prospectively enrolled, including 20 PCR-confirmed VZV-positive patients and 10 PCR-negative controls (Fig. 2). These conditions are often challenging to distinguish based solely on clinical examination. The VZV group included 19 patients with herpes zoster and 1 with varicella, all confirmed by positive VZV PCR results from blister fluid specimens. The control


**Fig. 2** Clinical manifestations of participants in the VZV or control groups. (A) Adult varicella [VZV group]. (B) Herpes zoster ophthalmicus [VZV group]. (C) Herpes zoster on the lower lip confirmed by a positive VZV PCR result, mimicking herpes simplex labialis [VZV group]. (D) Herpes simplex one left buttock with neuralgia, mimicking herpes zoster, with a negative VZV PCR result and viral culture revealed HSV [control group]. (E) Early stage of herpes zoster confirmed by a positive VZV PCR result, only presented with one painless erythematous plaque with some tiny vesicles [VZV group]. (F) Contact dermatitis with bullous formation, mimicking the early stage of herpes zoster [control group].

group included five patients with bullous pemphigoid, three with bullous contact dermatitis, one with herpes simplex, and one with noninfectious vesiculobullous lesions, all confirmed negative for VZV by PCR.

PCR confirmation of VZV infection was performed using a LabTurbo Virus Mini Kit (Cat. No. LVN480-300) for DNA extraction, followed by amplification with a LightMix® varicella-zoster virus detection kit (Cat. No. 40-0211-32; Roche Diagnostics) in combination with a LightCycler® FastStart DNA Master HybProbe (Cat. No. 03-003-248-001). The assay targets a 290 bp fragment of gene 28 within the VZV genome and employs a LightCycler Red 640-labeled probe for fluorescence detection. An internal positive control (IC; 300 bp), labeled with LightCycler Red 690, was included to monitor amplification performance. Amplification was performed on a LightCycler platform according to the manufacturer's instructions. A cycle threshold ($C_t$) value $\leq 37$ was defined as positive, while samples with $C_t$ values between 37 and 40 were re-tested for confirmation.

Blister fluid was collected using sterile cotton swabs for ruptured vesicles and sterile droppers for intact ones. Swab samples were immersed in 1 mL of viral transport medium. The swab was pressed against the inner wall of the tube several times and left in the medium for at least 5 minutes to promote antigen release. Blister fluid samples were stored at −20 °C after collection and thawed once prior to analysis. No repeated freeze–thaw cycles were performed. Four drops (approximately 0.2 mL) of each blister fluid sample were loaded into the sample well (S), and capillary action enabled lateral migration of the sample through the conjugate and detection zones. After 15 minutes, the results were visually interpreted according to the presence of colored lines: a positive result was defined as visible bands on both the test (T) and control (C) lines, a negative result as a single band on the C line only, and an invalid result as the absence of the C line. The study protocol was reviewed and approved by the Institutional Review Board of Chang Gung Memorial Hospital (IRB No.: 202001996A3). Written informed consent was obtained from each participant or legal guardian.

### Reflectance spectral quantification of clinical samples

The same spectrum analyzer described above was employed for quantitative evaluation of VZV antigen levels in patient blister fluid samples. Reflectance spectral analysis was performed using an optical reader to obtain $\alpha$ values, defined as the ratio of reflectance intensity at 650 nm to the minimum reflectance within the 430–600 nm range. The $\alpha$ values obtained from clinical test strips were statistically compared between PCR-confirmed VZV-positive and control groups.

Diagnostic performance was assessed using receiver operating characteristic (ROC) curve analysis to determine the optimal cut-off value and corresponding sensitivity, specificity, and area under the curve (AUC). A two-tailed $p$-value $<0.05$ was considered statistically significant.

### Smartphone-based colorimetric quantitative analysis

To provide an equipment-free alternative, a smartphone-based colorimetric system was established. Using a smartphone camera and the free "ColorPicker" application, red/green/blue (RGB) values were extracted from photographs of the test strips. All photographs were taken in a mini photo studio equipped with a standardized 5000 K LED lighting system to ensure uniform illumination and minimize color bias. After obtaining the RGB color values of the T-line, C-line, and the blank area of the test strip, a grayscale value of each area was estimated by the formula gray = R × 0.299 + G × 0.587 + B × 0.114. The TC value was defined as the grayscale ratio between the T line and C line, and the TB value as the ratio between the T line and background blank region. ROC curve analysis of TC and TB values determined the optimal cut-off points, sensitivity, and specificity, enabling semi-quantitative assessment without specialized instruments.

## Results and discussion

To systematically evaluate the performance and clinical applicability of the blister fluid-based VZV rapid test, we assessed its analytical sensitivity, reproducibility, and diagnostic performance across multiple readout modalities. The results are presented in a stepwise manner, beginning with *in vitro* analytical characterization to define detection limits, followed by visual and quantitative evaluation in clinical blister fluid samples, and concluding with the assessment of a smartphone-based, instrument-free readout. This integrated analysis enables direct comparison between visual interpretation and quantitative approaches, and provides a comprehensive framework for interpreting assay performance in real-world clinical settings.

### *In vitro* analytical performance of the VZV rapid test strip

To characterize the analytical performance of the VZV rapid test strip, serial dilutions of purified VZV glycoprotein antigen (0–800 pg mL$^{-1}$) were applied and quantified using a reflectance spectrum-based optical reader. All test strips consistently displayed a visible control (C) line, confirming suitable assay function (Fig. 3). The test (T) line demonstrated progressively reduced color intensity with decreasing antigen concentrations and became visually indistinguishable at concentrations below approximately 200 pg mL$^{-1}$, defining the practical limit of naked-eye interpretation.

Quantitative reflectance spectral analysis revealed a strong linear correlation between $\alpha$ values and antigen concentrations across the tested range ($R^2$ = 0.9527; Fig. 3). Using the blank mean and standard deviation, the calculated LOD and LOQ were 1.48 pg mL$^{-1}$ and 42.9 pg mL$^{-1}$, respectively. These values indicate that spectrum-based optical analysis substantially extends detection sensitivity beyond the threshold achievable by visual inspection alone,

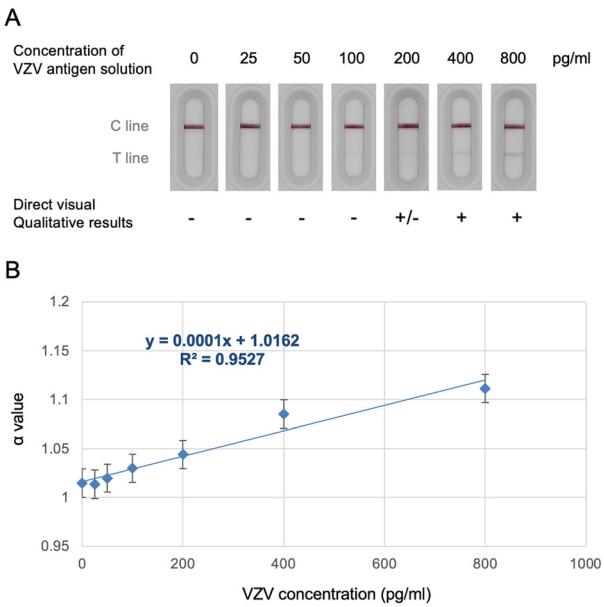


**Fig. 3** *In vitro* performance of the VZV rapid test strip. (A) Representative images of test strips loaded with VZV antigen solutions (0–800 pg $mL^{-1}$). Visible T-line development was observed from approximately 200 pg $mL^{-1}$, while C-lines remained consistently detectable. (B) Reflectance spectral analysis demonstrated a linear increase in $\alpha$ values with antigen concentration ($y$ = 0.0001$x$ + 1.0162, $R^2$ = 0.9527). Error bars indicate the standard deviation from triplicate measurements.

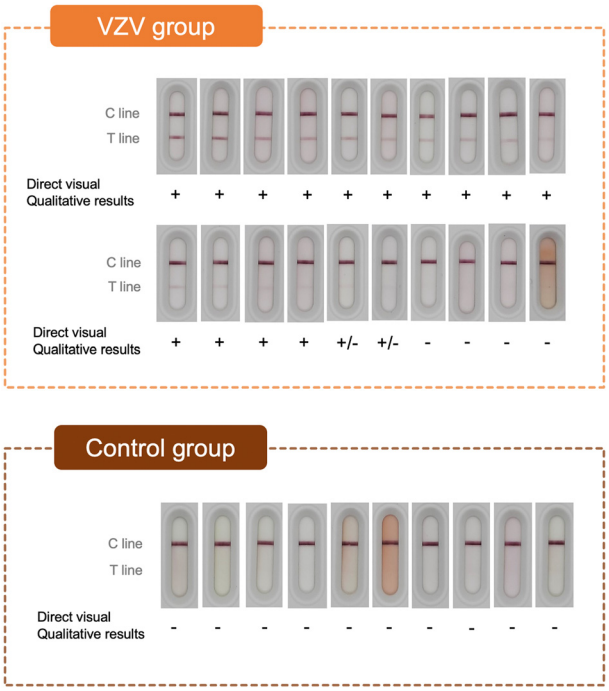


**Fig. 4** Real-world testing using blister fluid samples for VZV rapid test strips. Sensitivity and specificity by direct visual interpretation were 80% and 100%, respectively.

enabling reliable quantification at concentrations well below visual detectability.

To assess assay reproducibility, triplicate measurements were performed at each antigen concentration. The $\alpha$ values exhibited minimal variation, with coefficients of variation (CV%) ranging from 0.04% to 0.83%, demonstrating excellent intra-assay repeatability. This high reproducibility supports the robustness of the spectral quantification approach and its suitability for downstream clinical application.

Together, these analytical results define the practical limit of visual detection and demonstrate the advantage of quantitative spectral analysis in extending sensitivity beyond this threshold. This analytical framework therefore serves as a reference for interpreting visual and quantitative readouts in subsequent analyses of clinical blister fluid samples.

### Visual qualitative interpretation of clinical blister fluid samples

Clinical blister fluid samples produced interpretable visual results within 15 minutes (Fig. 4), consistent with real-world point-of-care requirements. Among 20 PCR-confirmed VZV-positive cases, 16 (80%) demonstrated both test (T) and control (C) lines and were therefore classified as positive. Of these, 14 showed clearly visible T lines, whereas two exhibited faint T lines that could be challenging to interpret by visual inspection alone. All 10 PCR-negative control samples displayed only C lines, resulting in a specificity of 100%. When compared with PCR, the assay achieved a sensitivity of 80%, specificity of 100%, and an overall diagnostic accuracy of 86.7% (26/30).

The observed visual performance should be interpreted in the context of current diagnostic options for VZV, which remain constrained by procedural complexity, infrastructure requirements, and turnaround times that are often incompatible with the narrow therapeutic window for antiviral therapy. Conventional laboratory techniques—including Tzanck smear, PCR, direct immunofluorescence (DIF) staining, serology, and viral culture—each present distinct limitations in routine clinical workflows. The Tzanck smear, historically the most accessible point-of-care test for vesicular eruptions, relies on cytologic identification of multinucleated giant or ballooned cells from blister fluid or ulcer base samples.[18,19] However, its diagnostic utility for VZV is limited by highly variable sensitivity (32–80%), strong operator dependence, inability to distinguish VZV from herpes simplex virus (HSV), and the requirement for microscopy facilities.[18,20]

Although PCR remains the diagnostic gold standard for VZV with excellent analytical performance,[21] it requires specialized laboratory infrastructure and trained personnel and may not be readily available in low-resource or urgent-care settings. DIF staining provides moderately high sensitivity (82–87%) and specificity (76%),[19,22] but involves labor-intensive sample preparation and is less effective for VZV than for HSV. Serological assays detecting VZV-specific IgG are inherently retrospective, reflecting prior exposure rather than active infection,[19] while viral culture, although

highly specific, suffers from extremely low sensitivity (~20%) and prolonged turnaround times.[19] Collectively, these constraints underscore the persistent lack of a truly practical, non-invasive, and rapid point-of-care diagnostic for VZV in real-world clinical settings.

From a clinical perspective, differentiation between VZV and HSV remains particularly challenging, as both viruses belong to the *Herpesviridae* family[23] and frequently present with overlapping cutaneous manifestations, including localized pain and grouped vesicles due to latent reactivation. Their glycoprotein profiles are highly homologous,[24] further complicating clinical discrimination. Notably, the Tzanck smear cannot distinguish between these two viruses.[19] In the present preliminary evaluation, HSV-positive samples were included as controls, and no positive signal was observed in these samples. Although limited in number, this finding suggests that the assay is capable of distinguishing VZV from HSV under the evaluated conditions, thereby supporting more appropriate antiviral selection and dosing at the point of care.

In parallel with these conventional diagnostic approaches, several rapid testing strategies for VZV have been reported over the past three years, each addressing specific clinical needs while presenting inherent trade-offs. Antibody-based LFAs targeting VZV IgG from fingerstick blood provide rapid assessment of serostatus, but are unable to differentiate active infection from past exposure.[25] Antigen-based colloidal gold LFAs detecting VZV gE protein from vesicular fluid achieve high specificity; however, their reported detection limit (~30 ng $mL^{-1}$)[26] remains substantially higher than the analytical sensitivity achieved in the present study (LOD = 1.48 pg $mL^{-1}$; LOQ = 42.9 pg $mL^{-1}$). Molecular approaches—including recombinase-aided amplification with lateral flow (RAA-LF),[27] CRISPR/Cas12a systems combined with quantum dot nanobead LFAs,[28] and one-pot LbCas12a-RPA-LFT platforms[29]—offer remarkable analytical sensitivity, in some cases detecting as few as 3–5 genomic copies per reaction within 25–60 minutes. Nevertheless, these methods require specialized reagents, temperature-controlled amplification, and multiple handling

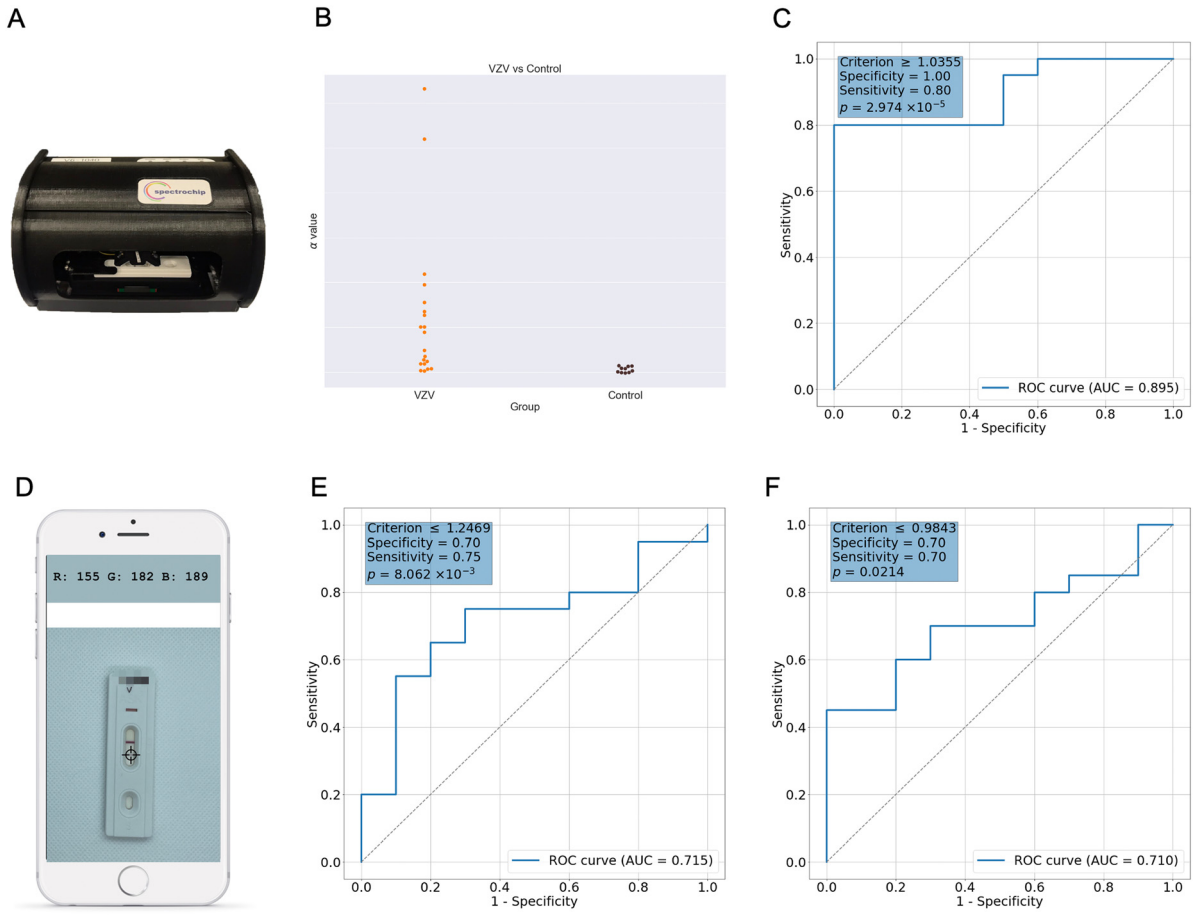


**Fig. 5** Quantitative assessment of VZV rapid test strips using spectrum-based optical analysis and smartphone colorimetry. (A) Spectrum-based optical reader employed for reflectance measurement of test strips. (B) Distribution of $\alpha$ values from clinical blister fluid samples, demonstrating significantly higher values in PCR-confirmed VZV-positive cases compared with controls ($p$ = 0.006). (C) Receiver operating characteristic (ROC) curve of $\alpha$ values, indicating an optimal threshold of 1.0355 with 80% sensitivity and 100% specificity (AUC = 0.895). (D) Smartphone-based RGB extraction method for colorimetric evaluation. (E) ROC curve of TC grayscale ratios (T-line/C-line), yielding 75% sensitivity and 70% specificity (AUC = 0.715). (F) ROC curve of TB grayscale ratios (T-line/background), showing 70% sensitivity and 70% specificity (AUC = 0.710).

steps, which may limit their scalability and routine deployment in decentralized or resource-limited settings.

### Reflectance spectral quantification of clinical blister fluid samples

Quantitative evaluation of clinical blister fluid samples was performed using the same reflectance spectral analysis approach. As shown in Fig. 5A–C, $\alpha$ values were significantly higher in the PCR-confirmed VZV-positive samples than in the control group ($p$ = 0.006). Receiver operating characteristic (ROC) curve analysis identified an optimal $\alpha$ cut-off value of 1.0355, corresponding to an estimated antigen concentration of approximately 193 pg mL$^{-1}$ based on the linear regression model.

At this threshold, spectral analysis achieved a sensitivity of 80% and a specificity of 100%, with an area under the curve (AUC) of 0.895 ($p$ = 1.974 × 10$^{-5}$). Notably, the quantitative cut-off (~193 pg mL$^{-1}$) closely aligned with the minimal concentration detectable by visual inspection (~200 pg mL$^{-1}$), supporting strong internal consistency between visual and quantitative readouts. Estimated VZV antigen concentrations in blister fluid varied markedly among patients, reaching levels as high as 12 476 pg mL$^{-1}$, reflecting substantial heterogeneity in viral burden during active infection.

Historically, the absence of point-of-care tests capable of estimating viral burden within blister fluid has limited real-time assessment of patient infectivity. This limitation is clinically relevant not only for individual patient management, but also for protecting close contacts—particularly unvaccinated infants and individuals without prior varicella infection—who may be susceptible to transmission from virus-containing vesicular fluid. By enabling semi-quantitative assessment of viral antigen levels at the point of care, the present approach offers a potential framework for more informed infection control considerations in both clinical and household settings.

In addition, this quantitative framework reduces reliance on subjective visual interpretation and enables more consistent classification of borderline or faint test results. Importantly, the close agreement between the quantitative cut-off and the visually detectable threshold supports the use of spectral analysis as an objective adjunct, rather than a replacement, to visual readout.

### Smartphone-based colorimetric quantitative analysis

To explore an instrument-free alternative suitable for decentralized or resource-limited settings, a smartphone-based colorimetric analysis was evaluated. RGB-derived grayscale ratios were calculated using both T-line/C-line (TC) and T-line/background (TB) metrics (Fig. 5D–F). Receiver operating characteristic (ROC) analysis using the TC metric yielded a sensitivity of 70%, a specificity of 75%, and an area under the curve (AUC) of 0.715 ($p$ = 0.00806) at an optimal cut-off value of 1.2469. Analysis based on the TB metric demonstrated comparable performance, with a sensitivity of 70%, a specificity of 70%, and an AUC of 0.710 ($p$ = 0.0214) at a cut-off value of 0.9843.

Although the smartphone-based approach showed lower diagnostic performance than the dedicated spectral reader, it provided reproducible semi-quantitative information without the need for specialized equipment. This trade-off between analytical precision and operational simplicity highlights the potential role of smartphone-assisted analysis as a practical adjunct for point-of-care or home-based testing scenarios. In this context, smartphone-based analysis may be particularly useful for initial screening or follow-up monitoring, where ease of access and rapid availability are prioritized over maximal analytical precision.

### Clinical and translational implications

Early-stage VZV infection often presents with nonspecific vesicular eruptions that overlap with a range of other blistering disorders, while many existing diagnostic modalities require laboratory infrastructure and turnaround times that exceed the narrow therapeutic window for effective antiviral intervention. In this real-world pilot validation, the blister fluid-based lateral flow assay demonstrated clinically actionable performance within minutes, enabling both qualitative and quantitative detection of VZV at the point of care.

The present work is distinguished by three key features that emphasize clinical applicability. First, the assay was purposefully designed for real-world use and validated in an unselected patient cohort that included both varicella and herpes zoster, using blister fluid as a non-invasive, liquid biopsy-like sample source. Second, the platform incorporates three complementary readout modalities—direct visual interpretation, quantitative spectral analysis, and smartphone-based assessment—providing flexibility for implementation across diverse healthcare settings, ranging from tertiary medical centers to rural clinics and home-based testing environments. Third, despite its procedural simplicity, the assay achieved robust diagnostic performance, with a sensitivity of 80% and a specificity of 100%, while delivering an analytical limit of detection markedly lower than that reported for comparable antigen-based lateral flow assays.

From a translational perspective, although ultra-sensitive molecular assays remain indispensable for certain research applications and low-viral load scenarios, their operational complexity currently constrains widespread use outside well-equipped laboratories. By contrast, the blister fluid-based VZV rapid test presented here represents a pragmatic balance between analytical performance and practical applicability. Its ability to provide rapid, bedside-compatible, and non-invasive VZV detection directly addresses a critical gap in current clinical workflows, facilitating timely antiviral initiation, complication

prevention, and infection control—particularly in settings where conventional laboratory infrastructure is unavailable.

The primary clinical benefit of a rapid VZV diagnostic lies in enabling prompt therapeutic intervention. Early antiviral treatment in herpes zoster has been shown to shorten disease duration, reduce rash progression, and significantly alleviate acute pain, thereby lowering the risk of PHN and improving patient quality of life. Timely diagnosis also helps prevent serious complications, including bacterial superinfection and ocular, pulmonary, or central nervous system involvement, especially in immunocompromised individuals or those with extensive disease. Furthermore, early identification of VZV infection may shorten the contagious period and reduce transmission risk, which is particularly important for unvaccinated or otherwise susceptible populations.

Blister fluid examination offers a minimally invasive alternative to traditional skin biopsy or blood-based testing and parallels the concept of "liquid biopsy" widely adopted in oncology.[30] Skin biopsy can be painful, requires specialized expertise, and may result in permanent scarring, while blood-based assays may not accurately reflect local viral activity within skin lesions. In contrast, blister fluid sampling is rapid, accessible, and well suited to point-of-care workflows. When integrated with lateral flow immunoassay technology, this "blister fluid biopsy" approach may be extended beyond VZV to other vesiculobullous disorders and adapted for use with cerebrospinal or vitreous fluids, potentially aiding in the diagnosis of central nervous system or ocular VZV infections.[4,31]

### Limitations

As a pilot study, the modest sample size may limit generalizability, and the control cohort could be expanded to further evaluate cross-reactivity, particularly with HSV-positive cases. Visual interpretation of lateral flow assays remains subject to inter-observer variability, especially for faint or borderline test lines, which may be mitigated through quantitative spectral or smartphone-assisted readouts in future iterations. The use of blister fluid as a diagnostic substrate also has practical constraints. Blister fluid volume and composition may vary by lesion stage and patient factors, and in late-stage or minimally exudative lesions, the obtainable fluid may be limited, potentially affecting test performance. Accordingly, this approach is the most applicable during active vesicular stages of infection. To enable earlier diagnosis in prevesicular lesions, our laboratory is developing microneedle-based interstitial fluid extraction integrated with the VZV rapid test for future applications. In addition, quantitative PCR data were not available for direct correlation with antigen levels in all samples, and longitudinal changes in blister fluid viral burden were not assessed. Larger, multi-center studies incorporating algorithm-assisted analysis and serial sampling will be essential to validate clinical performance across diverse settings.

## Conclusions

This study provides early evidence that a blister fluid-based, non-invasive VZV rapid test strip can deliver clinically meaningful diagnostic performance within minutes, without reliance on laboratory infrastructure. By integrating visual, spectral, and smartphone-based readouts, the platform balances sensitivity, specificity, speed, and operational simplicity, supporting its potential role as a scalable point-of-care tool for timely VZV diagnosis and management. Beyond its immediate diagnostic utility, this work highlights blister fluid as a practical and accessible substrate for point-of-care testing and introduces a "blister-fluid biopsy" paradigm that may be extended to other vesiculobullous skin diseases.

## Author contributions

Conceptualization: F. Y. W. and C. M. C.; methodology: F. Y. W., Y. Y. H., and C. M. C.; investigation: F. Y. W., Y. Y. H., and C. M. C.; formal analysis: F. Y. W. and C. M. C.; resources: F. Y. W., Y. Y. H., and C. M. C.; data curation: F. Y. W. and C. M. C.; writing – original draft: F. Y. W.; writing – review & editing: F. Y. W., Y. Y. H., and C. M. C.; visualization: F. Y. W.; supervision: C. M. C. and Y. Y. H.

## Conflicts of interest

All authors state that there are no conflicts to declare.

## Data availability

The data that support the findings of this study are available from the corresponding authors upon reasonable request, subject to privacy and ethical restrictions.

## Acknowledgements

This work was supported by Taiwan's National Science and Technology Council [grant number 113-2222-E-182-003-MY2 & 113-2221-E-007-021-MY3] and Chang Gung Memorial Hospital, Linkou, Taiwan [grant number CMRPGBL0021].

## References

1 A. M. Arvin, *Clin. Microbiol. Rev.*, 1996, **9**, 361–381.
2 A. A. Gershon, J. Breuer, J. I. Cohen, R. J. Cohrs, M. D. Gershon, D. Gilden, C. Grose, S. Hambleton, P. G. Kennedy, M. N. Oxman, J. F. Seward and K. Yamanishi, *Nat. Rev. Dis. Primers*, 2015, **1**, 15016.
3 A. R. Davis and J. Sheppard, *Eye & Contact Lens*, 2019, **45**, 286–291.
4 M. A. Nagel and D. Gilden, *Curr. Treat Options Neurol.*, 2013, **15**, 439–453.
5 J.-H. Kang, J.-J. Sheu and H.-C. Lin, *Clin. Infect. Dis.*, 2010, **51**, 525–530.

6 M. Marin, D. Güris, S. S. Chaves, S. Schmid and J. F. Seward, *MMWR Recomm. Rep.*, 2007, **56**, 1–40.
7 M. Marin, J. Leung and A. A. Gershon, *Pediatrics*, 2019, **144**(3), e20191305.
8 R. Harpaz, I. R. Ortega-Sanchez and J. F. Seward, *MMWR Recomm. Rep.*, 2008, **57**, 1–30, quiz CE32-34.
9 P. Bhalla, G. N. Forrest, M. Gershon, Y. Zhou, J. Chen, P. LaRussa, S. Steinberg and A. A. Gershon, *Clin. Infect. Dis.*, 2015, **60**, 1068–1074.
10 C. Warren-Gash, H. Forbes and J. Breuer, *Expert Rev. Vaccines*, 2017, **16**, 1191–1201.
11 S. Yeh, B. Ahmed, N. Sami and A. R. Ahmed, *Dermatol. Ther.*, 2003, **16**, 214–223.
12 R. W. Johnson, *Expert Rev. Vaccines*, 2010, **9**, 21–26.
13 A. A. Gershon and M. D. Gershon, *Clin. Microbiol. Rev.*, 2013, **26**, 728–743.
14 S. Tyring, R. A. Barbarash, J. E. Nahlik, A. Cunningham, J. Marley, M. Heng, T. Jones, T. Rea, R. Boon and R. Saltzman, *Ann. Intern. Med.*, 1995, **123**, 89–96.
15 C. Mo, J. Lee, M. Sommer, C. Grose and A. M. Arvin, *Virology*, 2002, **304**, 176–186.
16 K. M. Koczula and A. Gallotta, *Essays Biochem.*, 2016, **60**, 111–120.
17 S. W. Lin, C. F. Shen, C. C. Liu and C. M. Cheng, *Front. Bioeng. Biotechnol.*, 2021, **9**, 752681.
18 G. T. Nahass, B. A. Goldstein, W. Y. Zhu, U. Serfling, N. S. Penneys and C. L. Leonardi, *JAMA, J. Am. Med. Assoc.*, 1992, **268**, 2541–2544.
19 A. Sauerbrei, U. Eichhorn, M. Schacke and P. Wutzler, *J. Clin. Virol.*, 1999, **14**, 31–36.
20 E. Folkers, A. P. Oranje, J. N. Duivenvoorden, J. P. van der Veen, J. U. Rijlaarsdam and J. A. Emsbroek, *Genitourin. Med.*, 1988, **64**, 249–254.
21 R. Harbecke, M. N. Oxman, B. A. Arnold, C. Ip, G. R. Johnson, M. J. Levin, L. D. Gelb, K. E. Schmader, S. E. Straus, H. Wang, P. F. Wright, C. T. Pachucki, A. A. Gershon, R. D. Arbeit, L. E. Davis, M. S. Simberkoff, A. Weinberg, H. M. Williams, C. Cheney, L. Petrukhin, K. G. Abraham, A. Shaw, S. Manoff, J. M. Antonello, T. Green, Y. Wang, C. Tan and P. M. Keller, *J. Med. Virol.*, 2009, **81**, 1310–1322.
22 B. Kleinschmidt-DeMasters and D. H. Gilden, *Arch. Pathol. Lab. Med.*, 2001, **125**, 770–780.
23 I. Steiner, *Immunol. Rev.*, 1996, **152**, 157–173.
24 C. Grose, *Rev. Infect. Dis.*, 1991, **13**, S960–S963.
25 N. Vafai, K. Self, B. Sheffield, S. Hojvat, A. Kusi-Appiah, P. Vaughan, E. Cowan and A. Vafai, *J. Immunol. Methods*, 2023, **514**, 113429.
26 A. Wang, Y. Niu, J. Zhao, H. Liu, P. Ding, Y. Chen, J. Zhou, X. Zhu, Y. Zhang, C. Liang and G. Zhang, *Virology*, 2023, **586**, 35–42.
27 K. M. Bienes, L. Mao, B. Selekon, E. Gonofio, E. Nakoune, G. Wong and N. Berthet, *Diagnostics*, 2022, **12**(12), 2957.
28 X. Zhong, Q. Fu, Y. Wang, L. Long, W. Jiang, M. Chen, H. Xia, P. Zhang and F. Tan, *Appl. Microbiol. Biotechnol.*, 2023, **107**, 3319–3328.
29 Y. Huang, X. Zhang, N. Qi, W. Zhou, W. Zhu and L. Ji, *Microchem. J.*, 2025, **208**, 112445.
30 G. Poulet, J. Massias and V. Taly, *Acta Cytol.*, 2019, **63**, 449–455.
31 J. Garweg and M. Böhnke, *Clin. Infect. Dis.*, 1997, **24**, 603–608.